Control of multistate hopping intermittency

B. K. Goswami*
Laser and Plasma Technology Division, Bhabha Atomic Research Centre, Mumbai 400085, India
(Received 29 July 2008; published 11 December 2008)

In multistable regimes, noise can create "multistate hopping intermittency," i.e., intermittent transitions among coexisting stable attractors. We demonstrate that a small periodic perturbation can significantly control such hopping intermittency. By "control" we imply a qualitative change in the probability distribution of occupation in the phase space around the stable attractors. In other words, if the uncontrolled system exhibits a preference to stay around a given attractor (say "*A*") in comparison to another attractor (say "*B*"), the control perturbation creates a contrasting scenario so that attractor *B* is most frequently visited and consequently, the occupation probability becomes maximum around *B* instead of *A*. The control perturbation works in the following way: It destroys attractor *A* by boundary crisis while attractor *B* remains stable. As a result, even if the system is pushed by noise into the erstwhile basin of attractor *A*, the system does not remain there for long and therefore stays longer around attractor *B*. Significantly, such a change in the intermittent scenario can be obtained by a small-amplitude and slow-periodic perturbation. The control is theoretically demonstrated with two standard models, namely, Lorenz equations (for autonomous systems), and the periodically driven, damped Toda oscillator (for nonautonomous systems). Recent experiments with a cavity-loss modulated CO_2 laser and an analog circuit of Lorenz equations have validated our theoretical demonstrations excellently.

DOI: 10.1103/PhysRevE.78.066208 PACS number(s): 05.45.Ac, 42.65.Sf, 44.25.+f, 05.45.Gg

I. INTRODUCTION

Intermittency can be broadly defined as sustained intermittent transitions among qualitatively different types of dynamical behavior. Some well known examples are (i) Pomeau and Manneville (PM) types of intermittency [1], (ii) crisis-induced intermittency [2,3], and (iii) on-off intermittency [4]. In the case of symmetric multistable systems (like two-well potential Duffing oscillator [5] or cubic map [6]) crisis-induced intermittency occurs in the form of intermittent switching between two coexisting chaotic attractors. Various reports have established that crisis-induced intermittency (with or without noise) exhibits some scaling laws somewhat analogous to those of Feigenbaum sequence and PM intermittency [5–7].

Multistable systems that do not possess any symmetry can also exhibit intermittent jumps among coexisting attractors in the presence of noise [8]. Also, the attractors need not be chaotic and the number of such attractors could be arbitrary. The occurrence of intermittent jumps depends on the strength of noise, basin sizes, the nature of basin boundaries, and the time duration of the transient dynamics towards the attractor(s) [9]. In general, the threshold strength of noise required to knock the system out of a given attractor depends on the separation in the phase space between the attractor and the neighboring boundary saddle. Therefore the smaller the basin of attraction is, the more susceptible the system is to move out of the attractor. In contrast, the larger basins will be able to hold the system inside relatively for stronger noise [10]. When the noise is so strong that no basin can hold the system for long, it leads to intermittent hopping among coexisting attractors (henceforth referred to as "multistate hopping intermittency"). Notably, PM, on-off and crisis-induced intermittency occur in the close neighborhood of some local bifurcations or crises. In contrast, hopping intermittency can occur anywhere in the parameter space as long as the system remains multistable. Intermittent switching is a special case of hopping intermittency (in the case of symmetric multistable systems) that occurs when the coexisting chaotic attractors simultaneously collide with the common boundary saddle, resulting in the merger of the chaotic attractors in the phase space. The presence of adequately strong noise may advance the onset of such intermittent switching.

Numerous efforts have been made towards controlling PM, on-off, and crisis-induced intermittency. For instance, one may look into some reports on the control of on-off intermittency applying (i) a small feedback control [11], (ii) periodic modulation of system parameters [12], or (iii) by low-frequency noise [13]. Similarly, control of crisis-induced intermittency has also been demonstrated in the dynamics of a kicked, damped spin with the help of small, occasional changes of a system parameter [14]. Pomeau-Manneville type-I intermittency also exhibits qualitative changes under periodic perturbation of system parameters [15]. However, to our knowledge, no significant effort has been made so far to control multistate hopping intermittency.

In this paper, we demonstrate that a small periodic perturbation can successfully control such hopping intermittency. The perturbation could be in the form of modulation of any system parameters, or as a driving force. To verify the robustness of the control mechanism, we explore the dynamics of not only one trajectory but simultaneously a large number (say N_1) of trajectories over a suitably large phase-space region around the coexisting attractors. We divide this phase-space region into a large number (say N_2) of pixels (or cells) and simulate the dynamics of all trajectories for a large time interval (say N_3 suitably small time steps). Finally, we compute the occupation probability at any given pixel as the total number of visits in the pixel, normalized by $N_1N_2N_3$. By "control" we imply a qualitative change in the probability

*binoy@barc.gov.in

distribution of occupation in the phase space around the coexisting stable attractors. In other words, if the uncontrolled system exhibits preference to stay around a given attractor (say "*A*") in comparison to another attractor (say "*B*"), the control perturbation creates a contrasting scenario so that attractor *B* is visited most frequently and consequently, the occupation probability becomes maximum around attractor *B* instead of *A*. The control perturbation works in the following way: it leads to boundary crisis of attractor *A* while attractor *B* remains stable. As a result, even if the system is pushed by noise into the erstwhile basin of attractor *A*, the system does not remain there for long and preferentially remains around attractor *B*. Significantly, we demonstrate that such a control in the intermittent scenario can be obtained by a small-amplitude and slow-periodic perturbation.

Furthermore, keeping in mind the broad applicability of the control mechanism over a range of nonlinear systems of interest, we consider two standard models, Lorenz equations[1] and the Toda oscillator.[2] The Lorenz model can exhibit multistability by pitchfork and subcritical Hopf bifurcations. In this paper, we consider the case of multistability created by subcritical Hopf bifurcation. The Toda oscillator on its own does not exhibit Hopf bifurcation or multistability. However, in the presence of periodic force or parametric excitation, it can exhibit multistability due to overlap of more than one (sub)harmonic resonance [23,24] or recurrent period n-tupling ($n=3,4,5,\ldots$) phenomena [22,23]. By testing the control mechanism on the Lorenz model and the periodically forced Toda oscillator, we intend to verify its applicability among a broad variety of autonomous as well as periodically driven multistable systems, including class-C lasers, fluid dynamical systems, and parameter modulated class-B lasers.

The content of the paper is organized as follows. In Sec. II, we demonstrate the control of two-state intermittency in the case of the Toda oscillator that is driven by two periodic forces and Gaussian white noise. The primary force creates the bistable scenario (simultaneous coexistence in the phase space of period-1 and period-2 attractors). The noise induces intermittent jumps from period 2 to period 1 though the occupation probability remains maximum around period 2. Next we show that an additive secondary periodic force can create a completely contrasting scenario where the occupation probability becomes maximum around period 1 thus demonstrating controlled reduction of visits towards period 2. In Sec. III we demonstrate the control in the case of the Lorenz model. We operate in a parameter regime that exhibits coexistence of a chaotic attractor and two steady states. In the presence of adequately strong noise, the system intermittently jumps from the chaotic attractor to the steady states even though the occupation probability remains maximum around the saddle of the chaotic attractor. Here again we show that a small-amplitude periodic modulation of any system parameters creates a contrasting scenario where the occupation probability around the saddle drastically reduces. In comparison, the steady states become most preferred attractors.

II. CONTROL OF HOPPING INTERMITTENCY IN TODA OSCILLATOR DYNAMICS

The Toda oscillator is described by

$$\dot{X} = Y;$$

$$\dot{Y} = -\alpha Y - (e^X - 1) + F_d \cos(\omega_d \tau) + F_c \cos(\omega_c \tau + \phi) + \xi, \tag{1}$$

where F_d and ω_d are, respectively, the amplitude and frequency of the primary force ("drive"). F_c and ω_c are, respectively, the amplitude and frequency of the control perturbation. The phase term ϕ is introduced to take into account any possible phase difference between the drive and the control. ξ represents the Gaussian white noise of standard deviation σ. We consider the dissipativity $\alpha=0.015$ and drive frequency $\omega_d=1.95$. Figure 1(a) shows the bifurcation diagram with the drive amplitude as the control parameter. The period-1 state (denoted by "1") undergoes subcritical period doubling at point "D" and the system jumps to the period-2 state (denoted by "2"). If we follow the period-2 branch while reducing the drive amplitude, period 2 disappears via inverse saddle node bifurcation at the point "E." Thus one can notice the coexistence of period-1 and -2 attractors in the interval $0.1 \leqslant F_d \leqslant 0.3$ (denoted by ED). At any point in this interval, noise of adequate strength can create intermittent transitions between period 1 and 2. In Fig. 1(b), we consider $F_d=0.2$ as a typical example and show the basins of both the attractors, demarcated by the stable manifold (green and maroon curves in color online and dark lines in print) of the period-2 saddle ("S"). The unstable manifold (light blue curves in color online and gray lines in print) asymptotically approaches the period-1 and -2 attractors. The period-2 saddle and its manifolds are computed using Kawakami's algorithm [25]. In this plot, manifolds, stable, and saddle equilibriums have been shown after stroboscopic sampling with the sampling frequency ω_d. The basin boundary is smooth as there is no homoclinic intersection. The separation of the period-2 attractor from the period-2 boundary saddle ("S") is larger in comparison to that for the period-1 attractor. Therefore at low strength of noise, one may observe unidirectional transition from period 1 to period 2 but not the other way. We increase the standard deviation of noise until we observe reasonably frequent intermittent jumps. The time series in Fig. 1(c) shows such a case at standard deviation $\sigma=0.4$. The period-1 and -2 attractors are located on the horizontal arrows (denoted by "1" and "2", respectively). Since the basin of period-2 attractor is much larger in comparison to that of the period-1 attractor, the system remains in the vicinity of the period-2 attractor for much more time than that around period 1.

Next we introduce a slow-periodic control ($\omega_c=0.039$; $\omega_c \ll \omega_d$), and increase the control amplitude (F_c) gradually

[1]This model is a universally recognized paradigm of autonomous systems, including thermal fluid dynamics and class-C lasers like NH_3 [16] and Raman lasers [17].

[2]This oscillator may be considered as a paradigm of a large class of periodically forced nonlinear systems, including various class-B lasers [18,19] like CO_2, Nd-YAG, doped fiber, and semiconductor lasers, and oscillators [20]. Also it exhibits fascinating qualitative similarity with the Hénon map [21,22].

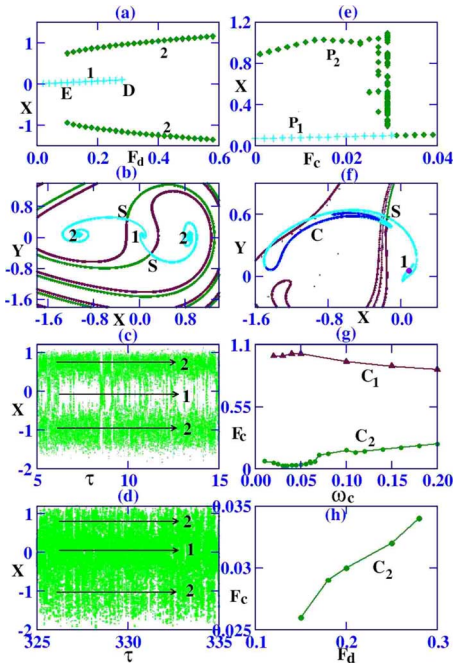

FIG. 1. (Color online) Control of two-state hopping intermittency in the Toda oscillator dynamics. (a) The bifurcation diagram with F_d as the control parameter shows the coexistence of period-1 and -2 attractors in the interval $0.1 \leqslant F_d \leqslant 0.3$ (denoted by "ED"). (b) The basins of period-1 and -2 attractors are demarcated by the stable manifold of the period-2 saddle ("S"). (c) The time trace $X(\tau)$ indicates that the system stays most of the time in the period-2 attractor and occasionally visits the period-1 basin; $\sigma=0.4$. (d) In the presence of control ($\omega_c=0.039$, $F_c=0.03$, $\phi=0.0$), the intermittent jumps exhibit a completely contrasting scenario. (e) The bifurcation diagram with F_c as the control parameter; $F_d=0.2$, $\omega_c=0.039$. The sampling frequency is equal to ω_c. The controlled period 2 (P_2) becomes chaotic via the sequence of period doubling. Eventually the chaotic attractor is destroyed via the boundary crisis at $F_c \cong 0.03$ and the system jumps to the controlled period-1 state (P_1). (f) The boundary crisis of the chaotic attractor ("C") in association with the homoclinic tangency at $F_c \cong 0.03$. (g) The parametric dependence of crisis thresholds of period-2 and -1 attractors; $F_d=0.2$. (h) The dependence of the crisis threshold of the period-2 attractor on the amplitude of the primary drive; $\omega_c=0.039$.

by a small magnitude. For $F_c > 0.03$, we observe a significant development, as one can notice from the time series in Fig. 1(d). The system visits the neighborhood of period 1 for much more time in comparison to that around the period-2 state. This is a completely contrasting scenario in comparison to the uncontrolled dynamics. The role of the control perturbation in creating such a fascinating effect can be understood by analyzing the noise-free case. The control mechanism works in two ways: On one side, the period-2 attractor (P_2) becomes chaotic via Feigenbaum sequence [see the bifurcation diagram in Fig. 1(e)]. On the other hand, the invariant manifolds of the saddle undergo metamorphoses that leads to a homoclinic tangency. We illustrate the scenario in Fig. 1(f) for $F_c \sim 0.03$. In this plot, manifolds, chaotic orbit, and equilibriums have been shown after stroboscopic sampling with the sampling frequency ω_c. The period-2 saddle is denoted by the point "**S**."[3] The unstable manifold components of this saddle are shown by light blue curves in color online and gray lines in print. One component that asymptotically converges to the period-1 attractor (denoted by the filled circle symbol "1," violet in color and black in print) qualitatively remains unchanged. In contrast, the other component undergoes significant transformation in the form of infinitely much stretching and folding. The chaotic attractor, shown by the dark blue curve in color online and dark curve in print, lies in the closure of the unstable manifold. The stable manifold components are shown by green and maroon curves in color online and dark lines in print. One may notice the homoclinic tangency of the manifolds that leads to the boundary crisis of the chaotic attractor. Consequently, past the crisis ($F_c > 0.03$) the system settles down at the period-1 state.

Indeed, the control mechanism perturbs the period-1 attractor as well. If we increase the control amplitude sufficiently large, period 1 will also eventually become chaotic and an interior crisis later will expand the chaotic attractor in the phase space. However, the threshold control amplitude of such a scenario is very much larger in comparison to that required for boundary crisis of the period-2 attractor. To explain this point further, let us denote the threshold control amplitude to create the interior crisis of the period-1 attractor by C_1. Similarly, the threshold control amplitude to create the boundary crisis of the period-2 attractor is denoted by C_2. In Fig. 1(g), we show the parametric dependence of these two threshold amplitudes, namely, C_1 (maroon curve in color) and C_2 (green curve in color) on the control frequency ω_c. The remaining system parameters are unchanged. We notice that $C_1 \gg C_2$ in the entire control frequency range. Therefore by suitable choice of the control parameter values, one can selectively destroy the period-2 attractor.[4] The control mechanism works in a similar way in the case of noise-induced hopping intermittency. Past the crisis, even if the noise triggers the system to move into the erstwhile basin of the period-2 attractor, the chaotic transient would not last there for long and the system would come back close to the period-1 attractor. This explains how the periodic perturbation controls the noise-induced hopping intermittency.

We now consider again the noise-free dynamics to explore how the threshold control amplitude (C_2) varies in the bistable window ["ED" in Fig. 1(a)]. Figure 1(h) shows the dependence of C_2 on the drive amplitude when the control frequency $\omega_c=0.039$. We find that the threshold control amplitude increases as one moves away from the inverse saddle node bifurcation point ["E" in Fig. 1(a)] towards the subcritical period doubling point ["D" in Fig. 1(a)]. This feature can be attributed to the phase-space separation between the P_2

[3]In what follows, we follow the convention of the uncontrolled case [Fig. 1(b)] to identify the controlled period-2 saddle, its invariant manifolds, and the controlled period-1 and -2 attractors. This is done so that one can easily compare the uncontrolled case [Fig. 1(b)] with the controlled one [Fig. 1(f)].

[4]If the control frequency is incommensurate with the drive frequency, the oscillator can become chaotic via quasiperiodic torus and strange nonchaotic attractor formation [26,27]. The chaotic attractor later is destroyed by boundary crisis.

attractor and the saddle. The saddle is closest to the P_2 attractor near the saddle node bifurcation condition. Therefore the threshold control amplitude (C_2) will be minimum near point E. As one moves towards subcritical period doubling, the phase-space separation between the period-2 attractor and saddle increases. This leads to an increase of the threshold control amplitude (C_2) as we have observed. Consequences are similar in the case of noise-induced hopping intermittency. The control amplitude, required to reduce the intermittent jumps to the period-2 basin, increases as one proceeds along the bistable window "ED" in Fig. 1(a) from the inverse saddle node bifurcation condition to subcritical period doubling.

So far, we have demonstrated the control of intermittent jumps with one trajectory. To show the robustness of the control mechanism, we now consider the case when the control is applied on a large number of trajectories ($N_1=400$) simultaneously, and for each trajectory, ϕ has been chosen randomly. The initial points of the trajectories are organized in a two-dimensional (20×20) array formation over the phase-space region ($-2<X<2;-2<Y<2$) that covers the period-2 as well as the period-1 attractors. First the simulations are carried out for a certain initial time period to take care of the transient relaxations, and then for an interval [N_3 periods of simulation cycles, each cycle ($=2\pi/\omega_d$) consists of 250 time steps of integration]. For this second interval we monitor the locations of the trajectories in the same phase-space region after stroboscopic sampling at the drive frequency ω_d. We divide the selected phase-space region in $N_2(=400\times400)$ pixels and compute the total number of visits in each pixel [say, $N(X,Y)$]. Thus the occupation probability at a given pixel around (X,Y), denoted by $D(X,Y)=\frac{N(X,Y)}{N_1N_2N_3}$. Since, D is usually small, in the three-dimensional plots of $D(X,Y)$ in Fig. 2, we show D scaled up by some suitable number. In each plot, the color bar and the vertical coordinate denote the occupation probability $D(X,Y)$. Figure 2(a) shows the uncontrolled scenario when the occupation probability is highest around the period-2 attractor, and much smaller around period 1. The preference of the period-2 attractor in comparison to period 1 is due to the relatively large basin of the period-2 attractor. Next we introduce the control modulation ($\omega_c=0.039$) and increase the control amplitude gradually. Figure 2(b) shows the effect of control modulation of amplitude $F_c=0.01$. The occupation probability around period 1 shows a significant improvement even though the probability remains maximum around period 2. At $F_c=0.02$ [Fig. 2(c)], the probability distribution exhibits a contrasting scenario, i.e., the probability is maximum around the period-1 attractor while the probability around the period-2 state is about half of that around the period-1 state. These observations suggest the occurrence of noise-induced boundary crisis at $F_c\cong0.02$ that is less than the deterministic threshold 0.03. This is because the crisis threshold reduces in the presence of noise [3]. Figure 2(d) shows the probability distribution when F_c is increased to 0.03. In comparison to the Fig. 2(c) scenario, the occupation probability around the period-1 attractor has increased further. This is because the lifetime of the chaotic transient reduces drastically as the value of F_c is increased even slightly beyond the threshold value. So the effect of control can be improved further by even a small increase of the control amplitude from the crisis value. Thus we confirm the ability of the control mechanism from the analysis of a large number of trajectories with random initial phases.

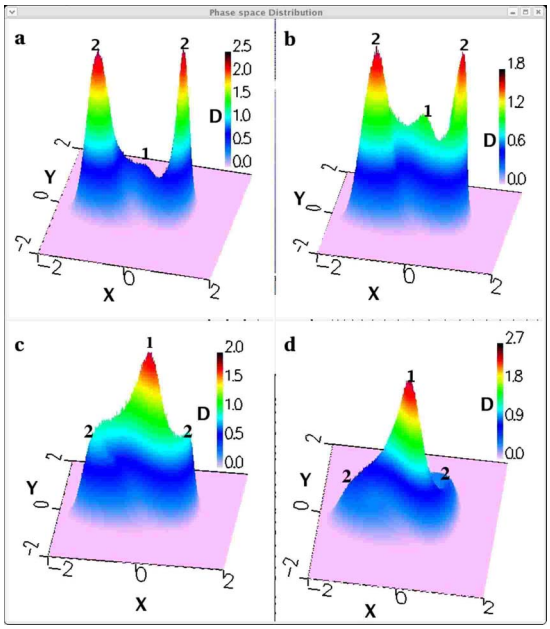

FIG. 2. (Color online) Demonstration of the control mechanism simultaneously over an ensemble of trajectories: $F_d=0.2$; $\sigma=0.6$. In the three-dimensional illustrations, phase-space occupation probability distribution $D(X,Y)$ is shown along the z coordinate and the color bar while the other two coordinates (X,Y) describe the phase space. (a) For an uncontrolled case, the occupation probability D is highest around the period-2 attractor (denoted by "2") and much less around period 1 (denoted by "1"). Plots (b)–(d) illustrate the probability distribution in the presence of noise and control signal with $F_c=0.01$, 0.02, 0.03, respectively. $\omega_c=0.039$. (b) At $F_c=0.01$, the occupation probability around period 1 increases significantly even though the probability around period 2 remains maximum. (c) At $F_c=0.02$, the occupation probability around period 1 is almost double that of period 2. (e) At $F_c=0.03$, the occupation probability around period 2 further declines. Consequently, the peak around period 1 increases further.

It is noteworthy that a small-amplitude periodic control can create such a fascinating qualitative change in the multistable scenario. Apparently it should be a tough proposition to make a system chaotic with a slow-periodic drive if the drive amplitude is small. To give a typical example, consider the case when the oscillator is driven only by a periodic force of frequency $\omega_d=0.04$ without any secondary control or noise. We have observed that the first period doubling occurs relatively at a large drive amplitude ($F_d>0.98$). This is because $\omega_d\cong0.039$ lies around the 50th period-2 subharmonic resonance region and it is known that higher order period-2 subharmonic resonances occur at increasingly large drive amplitude [20]. In sharp contrast, in the presence of the primary drive, the slow-periodic ($\omega_c=0.039$) control force leads to the Feigenbaum route to chaos and that too at a small amplitude ($F_c\cong0.03$). There are some similar reports on controlled destruction of attractors by periodic modulation of system parameters [28,29]. Pisarchik *et al.* [29] have sug-

gested that the threshold amplitude for the attractor destruction will be minimum when the control frequency is in the close vicinity of an eigenfrequency of that attractor. While this may be so for the creation of crisis of a chaotic attractor, one still needs to know how such a small amplitude could make a system chaotic, say via a sequence of period doubling. This can happen if the effective control amplitude is sufficiently large. We believe that such an enhancement of the effective control amplitude can occur due to the nonlinear interaction between the drive and the control. Also, the enhancement will be more prominent if either of the periodic forces (or both) belongs to some (sub)harmonic resonance region. We attempt to explain qualitatively in a few lines by analyzing the role of the primary drive (frequency ω_d) on the enhancement of the effective control amplitude. One can take into account the spectral line at frequency ω_c of any dynamic variables (say X or Y) and analyze how it undergoes enhancement due to the presence of the primary drive. Let us consider the case of the period-2 attractor whose spectrum is a Fourier series of frequency $\omega_d/2$. The additional presence of the control driving force (of frequency ω_c) creates sidebands around each spectral line of the uncontrolled attractor, in addition to generate a Fourier spectrum of ω_c. For instance, the spectral lines of frequencies $\omega_d/2 \pm \omega_c$ will be created around the line of frequency $\omega_d/2$. The nonlinearity of the oscillator creates further interactions between each of these side bands (say of frequency $\omega_d/2+\omega_c$) with the corresponding spectral line of frequency $\omega_d/2$, modifying the amplitude of the spectral line of frequency ω_c. Similarly, the interaction between the other side band (of frequency $\omega_d/2 - \omega_c$) and the line at $\omega_d/2$ will also contribute in the modification of the amplitude at ω_c. In the same way, the interactions among the higher-order spectral lines of the original spectrum (i.e., of frequency $n\omega_d/2; n>1$) with its side bands (of frequency $n\omega_d/2 \pm \omega_c$) will also contribute in modifying the amplitude at ω_c. The effective control amplitude will be maximum when all these terms are in phase. The effective amplification will have a resonant effect if either the drive or the control (or both) are in some (sub)harmonic resonance. In our case, the drive is in the period-2 subharmonic resonance. We believe this could provide some physical insight of the fascinating efficiency of the control perturbation in the presence of the drive.

III. CONTROL OF HOPPING INTERMITTENCY IN LORENZ MODEL DYNAMICS

Lorenz equations are described by

$$\dot{X} = -\sigma(X - Y),$$

$$\dot{Y} = rX - Y - XZ,$$

$$\dot{Z} = XY - bZ, \tag{2}$$

where σ, r, and b are well known Lorenz parameters. We fix $\sigma=10$, $b=1.2$, and observe multistability (coexistence of chaotic attractor with two steady states) in the interval $16.25 \leqslant r \leqslant 18.25$. For further details about the creation of

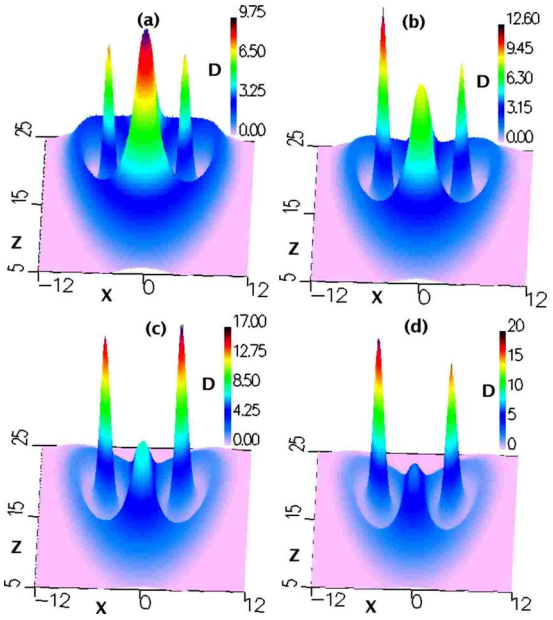

FIG. 3. (Color online) Control of hopping intermittency in the case of the Lorenz model; $r_0=17.15$, $\sigma=10$, $b=1.2$, $\lambda=5.0$. (a) In the absence of control, the occupation probability is highest around the saddle. The distribution also exhibits two maxima around the steady states. Plots (b)–(d) illustrate the probability distributions in the presence of control modulation over r with control frequency $\nu=0.8$ and $\delta=0.03$, 0.05, 0.07, respectively. As the control amplitude is increased, the occupation probability around the saddle (as well as the entire chaotic attractor) comes down. In contrast, the occupation probability around the steady states increases sharply. In other words, the intermittent visits to the chaotic attractor are controlled and the steady states become the most frequently visited attractors.

this multistable region, we refer to Fig. 1 and the associated discussions in Goswami [30]. As a typical example of control, we consider the operating condition in the middle of the multistable region at $r=17.15$, and introduce the Gaussian white noise (of zero mean) in the right-hand side of each equation. For simplicity, we also consider each noise generator having identical standard deviation (λ). Similar to the case of the Toda oscillator, we investigate the noise-induced intermittent transitions of a large number of trajectories ($N_1=400$) with initial points organized in a two-dimensional (20×20) array formation over the phase-space region ($-12<X<12; 5<Z<25$) that covers the chaotic attractor and the steady states. We simulate the dynamics of all trajectories for large number of time steps ($N_3 \sim 600\,000$) and compute the total occupation distribution of the trajectory points in the same phase-space region, divided in $N_2(=400\times400)$ pixels. Thus the probability distribution $D(X,Y)=\frac{N(X,Z)}{N_1N_2N_3}$. Since D is usually small, in the three-dimensional plots of $D(X,Z)$ in Fig. 3, we show D scaled up by some suitable number. Figure 3(a) shows the probability distribution for noise with standard deviation $\delta=5.0$. We observe that the occupation probability is highest around the saddle point ($X=0$, $Y=0$, $Z=0$). This plot also exhibits two peaks around the two stable steady states, thus indicating multistate intermittency. The peaks around the steady states

are separated from that of the chaotic attractor by unstable periodic orbits (UPOs) that define the basin boundaries. As we introduce the control modulation over r in the following form: $\{r=r_0[1+\delta\cos(2\pi\nu\tau)]$; $r_0=17.15$; $\nu=0.8\}$, and increase the control amplitude, the probability distribution undergoes a fascinating transformation. Figures 3(b)–3(d) show the probability distributions, respectively, for $\delta=0.003$, 0.005, 0.007. One clearly notices that as the control parameter value is increased, the occupation probability around the saddle comes down. In contrast, the probability sharply increases around the steady states. Figure 3(d) shows a contrasting scenario with respect to the uncontrolled case. The occupation probability around the saddle is much less in comparison to those around the steady states. In other words, the controlled scenario indicates that the steady states are more frequently visited than the chaotic attractor. This is a clear indication of the control on the noise-induced multistate intermittency. The underlying mechanism behind the control has some similarity with the Toda oscillator scenario. In the case of the Lorenz model, the chaotic attractor undergoes a boundary crisis due to the collision with the UPOs. We refer to Goswami [30] for further details about the controlled creation of the boundary crisis of the chaotic attractor by small periodic modulation of any system parameter. In fact, the threshold control amplitude (to create boundary crisis) could be reduced significantly if the control frequency is equal to or multiples of the frequency of the unstable periodic orbits. Under such circumstances, the UPOs undergo resonant evolutions in the phase space, resulting in the crisis. The UPO frequency for the given operating condition is 0.85 which is close to our control frequency. This could be one of the reasons for the crisis of the chaotic attractor at such a small modulation depth of the control. In a similar way, hopping intermittency can also be controlled by suitable modulation of any other system parameters. For instance, first we demonstrate the control by modulation over σ. For the uncontrolled scenario, we refer back to the case, shown in Fig. 3(a). Next we introduce the control modulation over σ in the following form: $\{\sigma=\sigma_0[1+\delta\cos(2\pi\nu\tau)]$; $r=17.15$, $\sigma_0=10$; $b=1.2$, $\nu=0.8\}$, and increase the control amplitude gradually. Figures 4(a) and 4(b) show the probability distribution for $\delta=0.02$ and 0.05, respectively. The control frequency $\nu=1.7$. As one can notice, at relatively small control amplitude, the saddle is the most frequently visited attractor [see Fig. 4(a)]. However, as δ is increased, a completely contrasting scenario occurs when the steady states become most frequently visited and the chaotic attractor the least. This implies that the chaotic attractor has been destroyed via boundary crisis, very similar to the case of control modulation over r, and the threshold modulation depth for the boundary crisis in the presence of noise is <0.05. Similarly, next we analyze the effect of periodic modulation over b of the following form: $\{b=b_0[1+\delta\cos(2\pi\nu\tau)]$; $r=17.15$, $\sigma_0=10$; $b=1.2$, $\nu=1.7\}$. Figures 4(c) and 4(d) illustrate the probability distribution for $\delta=0.003$, 0.01, respectively. Here again we find that with the increase of modulation over b, the occupation probability around the saddle significantly comes down while the peaks around the steady states become more prominent. Thus the threshold modulation depth for the boundary crisis in the presence of noise is <0.01. Also, we observe that any parameter can be modulated with a small-amplitude, periodic perturbation to control noise-induced multistate intermittency in the Lorenz model dynamics.

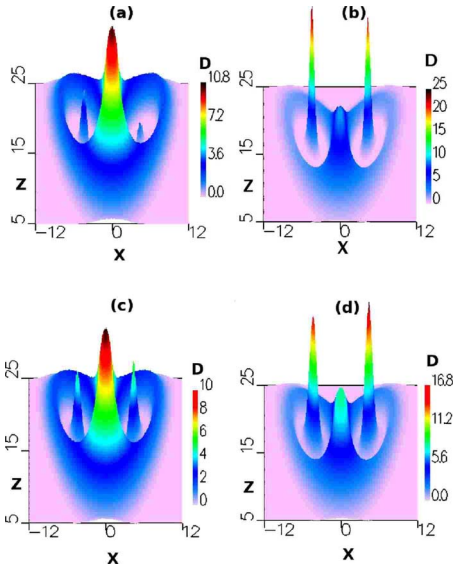

FIG. 4. (Color online) Demonstration of the control mechanism by periodic modulation over σ and b: $r_0=17.15$, $\sigma=10$, $b=1.2$, $\lambda=5.0$. (a) and (b) refer to σ modulation with $\delta=0.02$ and 0.05, respectively. The control frequency $\nu=1.7$. As the control amplitude is increased, the intermittent visits to the chaotic attractor, in particular, the saddle reduces significantly. On the contrary, the steady states are visited more frequently. (c) and (d) refer to b modulation with $\delta=0.003$ and 0.01, respectively. The control frequency $\nu=0.82$. Here again, one may notice that the little increase of control amplitude leads to a significant decrease of occupation probability over the chaotic attractor, and simultaneous increase of occupation probability around the steady states. These features are very similar to those for σ modulation.

We may note finally a few lines about our recent experiments [31] that have validated excellently the current theoretical demonstrations. In particular, we have carried out control experiments individually with an analog circuit of Lorenz equations and a bistable cavity-loss modulated CO_2 laser. The two-level laser rate equations model (and also the vibro-rotational model) of CO_2 laser may be reduced to the Toda oscillator model we studied in Sec. II. The periodic modulation of any system parameters (cavity loss, cavity length, or pump parameter) provides the driving force. Indeed, the CO_2 laser experiments are similar to our theoretical results. Similarly, the analog circuit experiments resemble those of Lorenz equations remarkably. We have analyzed the probability distribution of noise-induced multistate hopping intermittency first without control and then in the presence of control at various control amplitudes. The controlled scenario has been found very similar to our theoretical demonstrations.

To conclude, we have demonstrated that a small-amplitude periodic perturbation can control the noise-induced intermittent transitions among multiple coexisting attractors. These features are observed theoretically in two standard models, namely, Toda oscillator and Lorenz equations, and are recently validated experimentally.

We believe the control mechanism in the form of a small-amplitude slow periodic perturbation could also be advantageous for more complex systems that have several interdependent nonlinear subsystems. For instance, consider the network of nonlinear systems, (e.g., coupled array of lasers or electronic circuits) some of which can exhibit hopping intermittency. Similarly, we may think of the human body comprising nervous, circulatory, respiratory, and other systems whose functional properties are dynamically interdependent. Consider the case when one system exhibits intermittent jumps towards undesirable attractors, and the objective is to control the same without grossly affecting other systems. In such circumstances, a strong perturbation may not be preferable. Instead, we believe, the small-amplitude, slow-periodic perturbation would be of immense help and may be a necessary mechanism of control. This is because it may act selectively on the particular multistable system without perturbing other systems so significantly.

ACKNOWLEDGMENT

This work was supported by the Department of Atomic Energy, Government of India (11-R&D-BAR-4.11-0200: XI-N-R&D-26.09).

[1] Y. Pomeau and P. Manneville, Commun. Math. Phys. **74**, 189 (1980).
[2] C. Grebogi, E. Ott, F. Romeiras, and J. A. Yorke, Phys. Rev. A **36**, 5365 (1987).
[3] J. C. Sommerer, E. Ott, and C. Grebogi, Phys. Rev. A **43**, 1754 (1991); J. C. Sommerer, W. L. Ditto, C. Grebogi, E. Ott, and M. L. Spano, Phys. Rev. Lett. **66**, 1947 (1991).
[4] N. Platt, E. A. Spiegel, and C. Tresser, Phys. Rev. Lett. **70**, 279 (1993); P. W. Hammer, N. Platt, S. M. Hammel, J. F. Heagy, and B. D. Lee, *ibid.* **73**, 1095 (1994); Y.-C Lai and C. Grebogi, Phys. Rev. E **52**, R3313 (1995); M. Zhan and G. Hu, *ibid.* **62**, 375 (2000).
[5] F. T. Arecchi and F. Lisi, Phys. Rev. Lett. **49**, 94 (1982); F. T. Arecchi, R. Badii, and A. Politi, Phys. Rev. A **29**, 1006 (1984); F. T. Arecchi, R. Badii, and A. Politi, *ibid.* **32**, 402 (1985); Y. H. Kao, J. C. Huang, and Y. S. Gou, *ibid.* **35**, 5228 (1987).
[6] F. T. Arecchi, R. Badii, and A. Politi, Phys. Lett. **103A**, 3 (1984).
[7] M. Iansiti, Qing Hu, R. M. Westervelt, and M. Tinkham, Phys. Rev. Lett. **55**, 746 (1985); E. G. Gwinn and R. M. Westervelt, Phys. Rev. A **33**, 4143 (1986); S. J. Hahn, and K. H. Pae, Phys. Plasmas **10**, 314 (2003).
[8] M. Franaszek and L. Fronzoni, Phys. Rev. E **49**, 3888 (1994).
[9] S. Kraut and U. Feudel, Phys. Rev. E **66**, 015207(R) (2002).
[10] S. Kraut, U. Feudel, and C. Grebogi, Phys. Rev. E **59**, 5253 (1999).
[11] Y. Nagai, X.-D. Hua, and Y.-C. Lai, Phys. Rev. E **54**, 1190 (1996).
[12] R. J. Reategui and A. N. Pisarchik, Phys. Rev. E **69**, 067203 (2004).
[13] S. Aumaitre, F. Petrelis, and K. Mallick, Phys. Rev. Lett. **95**, 064101 (2005).
[14] K. Kacperski and J. A. Holyst, Phys. Rev. E **55**, 5044 (1997).
[15] J. M. Gac and J. J. Zebrowski, Phys. Rev. E **73**, 066203 (2006).
[16] C. O. Weiss and W. Klische, Opt. Commun. **51**, 47 (1984); C. O. Weiss and J. Brock, Phys. Rev. Lett. **57**, 2804 (1986); C. O. Weiss, N. B. Abraham, and U. Hübner, *ibid.* **61**, 1587 (1988); U. Hübner, N. B. Abraham, and C. O. Weiss, Phys. Rev. A **40**, 6354 (1989).
[17] R. G. Harrison, W. Lu, and P. K. Gupta, Phys. Rev. Lett. **63**, 1372 (1989); W. Lu and R. G. Harrison, Phys. Rev. A **43**, 6358 (1991).
[18] G. L. Oppo and A. Politi, Z. Phys. B: Condens. Matter **59**, 111 (1985); W. Lauterborn and R. Steinhoff, J. Opt. Soc. Am. B **5**, 1097 (1988); Y. Hori, H. Serizawa, and H. Sato, *ibid.* **5**, 1128 (1988); G.-L. Oppo, J. R. Tredicce, and L. M. Narducci, Opt. Commun. **69**, 393 (1989); Y. H. Kao, C. H. Tsai, and C. S. Wang, Rev. Sci. Instrum. **63**, 75 (1992); Y. H. Kao and H. T. Lin, Phys. Rev. A **48**, 2292 (1993).
[19] B. K. Goswami, Riv. Nuovo Cimento **28**, 1 (2005).
[20] C. Scheffczyk, U. Parlitz, T. Kurz, W. Knop, and W. Lauterborn, Phys. Rev. A **43**, 6495 (1991); U. Parlitz, Int. J. Bifurcation Chaos Appl. Sci. Eng. **3**, 703 (1993).
[21] E. Eschenazi, H. G. Solari, and R. Gilmore, Phys. Rev. A **39**, 2609 (1989).
[22] B. K. Goswami, Phys. Rev. E **62**, 2068 (2000); B. K. Goswami and S. Basu, *ibid.* **65**, 036210 (2002).
[23] B. K. Goswami, Opt. Commun. **122**, 189 (1996); Int. J. Bifurcation Chaos Appl. Sci. Eng. **5**, 303 (1995); **12**, 2691 (1997); Phys. Lett. A **245**, 97 (1998).
[24] V. N. Chizhevsky, J. Opt. B: Quantum Semiclassical Opt. **2**, 711 (2000); A. N. Pisarchik, Y. O. Barmenkov, and A. V. Kir'yanov, IEEE J. Quantum Electron. **39**, 1567 (2003).
[25] H. Kawakami, IEEE Trans. Circuits Syst. **31**, 248 (1984); T. Kurz and W. Lauterborn, Phys. Rev. A **37**, 1029 (1988).
[26] C. Grebogi, E. Ott, S. Pelican, and J. A. Yorke, Physica D **13**, 261 (1985); W. L. Ditto, M. L. Spano, H. T. Savage, S. N. Rauseo, J. Heagy, and E. Ott, Phys. Rev. Lett. **65**, 533 (1990); Y.-C. Lai, U. Feudel, and C. Grebogi, Phys. Rev. E **54**, 6070 (1996).
[27] *Strange Nonchaotic Attractors*, A. Pikovsky, S. Kuzentsov, and U. Feudel, World Scientific, Singapore, 2006.
[28] A. N. Pisarchik and B. K. Goswami, Phys. Rev. Lett. **84**, 1423 (2000); B. K. Goswami and S. Basu, Phys. Rev. E **66**, 026214 (2002).
[29] A. N. Pisarchik, Y. O. Barmenkov, and A. V. Kir'yanov, Phys. Rev. E **68**, 066211 (2003).
[30] B. K. Goswami, Phys. Rev. E **76**, 016219 (2007).
[31] B. K. Goswami, S. Euzzor, K. Al Naimee, A. Geltrude, R. Meucci, and F. T. Arecchi, *Experimental Chaos Conference*, 2008, Catania, Italy.